PO-0978 Histology correlation of in vivo [68Ga]PSMA-PET/MRI data of the prostate

K. Sandgren[1], J. Jonsson[1], T. Nyholm[1], S. Strandberg[1], M. Ogren[1], J. Axelsson[1], L. Blomqvist[1], B. Freidrich[2], A. Bergh[3], K. Ahlström Riklund[1], A. Windmark[1]
[1]University Umea Norrlands Universitetssjukhus, Radiation Sciences, Umea, Sweden
[2]University Umea Norrlands Universitetssjukhus, Surgical and Perioperative Sciences- Urology and Andrology, Umea, Sweden
[3]University Umea Norrlands Universitetssjukhus, Medical Biosciences, Umea, Sweden

Purpose or Objective

Image guidance is a cornerstone in individualized and targeted radiotherapy. However, there is still a need to perform a comprehensive analysis of which lesions are visible in the images. Preliminary results and a method to correlate histopathology to in vivo PET/MRI of prostate cancer is presented.

Material and Methods

Full diagnostic in vivo PSMA-PET/MRI (3T SIGNA GE) was performed on 8 patients prior to robot assisted radical prostatectomy.

Three-plane T2w MRIs were used to delineate prostate volumes. Individualized molds were created to preserve the in vivo shape and orientation of the prostate (fig. 1). All 3D-printed molds were created using a pre-created CAD model designed with 5 mm slits. The specimens were placed in their mold directly after each surgery. High resolution ex vivo T2w MRI of the fresh specimen was performed before formalin-fixation (within 90 minutes after the specimen left the patient´s body). The position of the MRI slices was localized according to the slits in the mold. The formalin-fixed specimen was sliced from the apex to base in 5 mm thick slices by the pathologist using the built-in slits in the mold. The standard procedure of PAD analysis was performed including paraffin embedding and microtoming in 5 µm thick slices. The histology slides were scanned with and without delineated Gleason score (GS), used to create GS specific maps. A 2D affine registration was used to register the histology to the ex vivo images on a slice by slice basis. The affine transform was used to account for specimen shrinkage during pathology preparations. The registered histology was then rigidly registered to the in vivo MRI using the ex vivo MRI as an intermediate.

In each patient, all lesions were categorized depending on size (<5 cm or >5 cm) and Gleason score. A visual non-blinded judgment of the lesion visibility using each imaging modality was performed. The judgement was done in consensus by two medical physicists, with the guidance of a radiologist.

Results

Our initial experience is that the procedure provides accurate mapping of pathological findings to in vivo PET/MRI data. GS maps can be co-registered to all included MRI sequences and PSMA PET. In the first 8 patients, 83 lesions were detected by the pathologist, see table 1.

Table 1: The number of lesions detected by the pathologist (histology) and the corresponding number of lesions detected in each imaging modality.

Gleason score <5 mm	**3+3**	**3+4**	**4+3**	**4+4**
Histology	41	8	10	0
T2w	0	0	0	0
ADC/DWI (b=1000 s/mm^2)	2	0	0	0
Ktrans	0	0	0	0
PSMA	1	1	1	0
mpMRI+PSMA	2	1	1	0

Gleason score >5 mm	**3+3**	**3+4**	**4+3**	**4+4**
Histology	1	8	14	1
T2w	0	5	4	0
ADC/DWI (b=1000 s/mm^2)	1	3	8	1
Ktrans	0	1	6	0
PSMA	0	4	5	1
mpMRI+PSMA	1	4	9	1

Conclusion

This is a time-efficient, non-expensive method in verifying image findings using histology. Our preliminary results suggest that combined PSMA-PET/mpMRI identifies more lesions than the individual imaging modalities.

PO-0979 Ultra-high field MRI for evaluation of rectal cancer stroma ex vivo: correlation with histopathology

T. Pham[1,2,3,4,5], T. Stait-Gardner[6], C.S. Lee[3,5,7], M. Barton[1,3,4], G. Liney[1,3,4], K. Wong[1,3,4], W. Price[3,6]
[1]Liverpool Cancer Therapy Centre- Liverpool Hospital, Radiation Oncology, Sydney, Australia
[2]Westmead- Blacktown and Nepean Hospitals, Radiation Oncology, Sydney, Australia
[3]University of New South Wales, Faculty of Medicine, Sydney, Australia
[4]Ingham Institute for Applied Medical Research, CCORE, Sydney, Australia
[5]Western Sydney University, School of Medicine, Sydney, Australia
[6]Western Sydney University and National Imaging Facility, Nanoscale Organisation and Dynamics Group, Sydney, Australia
[7]Liverpool Hospital, Anatomical Pathology, Sydney, Australia

Purpose or Objective

Current clinical MRI techniques in rectal cancer are unable to differentiate Stage T1 from T2 (invasion of muscularis propria) tumours, and the differentiation of tumour from desmoplastic reaction or fibrous tissue remains a challenge[1]. Diffusion tensor imaging (DTI) MRI has potential to assess collagen structure and organisation (anisotropy). To our knowledge, there have been no MRI studies assessing DTI MRI for rectal cancer ex vivo. The purpose of this study was to examine DTI MRI

derived biomarkers of rectal cancer stromal heterogeneity at high field strength ex vivo.

Material and Methods

Ten rectal tissue specimens were collected from 5 patients with a diagnosis of rectal cancer undergoing surgery through the Cancer Biobank. Two fresh specimens were collected from the surgical specimen of each patient: full thickness rectal cancer and full thickness adjacent normal rectum 5 – 10cm away from cancer. Tissue specimens were fixed in 10% formalin and embedded in 1% agarose containing 2mM gadopentetate dimeglumine for MR imaging. Tissue samples were scanned at 11.7 Tesla on the Bruker Avance II 500 MHz wide bore MRI. The MRI proctocol consisted of anatomical FLASH with 100 µm isotropic voxels, and functional DTI with 200 µm isotropic voxels and b-values 200, 800 and 3200 s/mm^2. Fractional Anisotropy (FA) values were calculated using the formula,

$$FA = \sqrt{\frac{3}{2}}\frac{\sqrt{(\lambda_1 - \langle\lambda\rangle)^2 + (\lambda_2 - \langle\lambda\rangle)^2 + (\lambda_3 - \langle\lambda\rangle)^2}}{\sqrt{(\lambda_1{}^2 + \lambda_2{}^2 + \lambda_3{}^2)}}$$

where the λ_1, λ_2, λ_3 and (λ) are the diffusion eigenvalues in three orthogonal directions and their average value, respectively. FA maps were generated with FA = 0 indicating isotropic diffusion (no organisation). The specimens were examined by light microscopy using H&E and Masson Trichome stains. Regions of interest were annotated on digital histopathology with a Pathologist, for correlation with DTI MRI.

Results

Examination of colour-encoded DTI and FA maps and corresponding histopathology demonstrated low colour signal intensity and low FA values (range 0.14 – 0.16) in tumour regions, indicating a lack of anisotropy and lack of stromal organisation in cancer. Heterogeneity within cancer stroma was seen on the DTI maps, with regions of moderate colour signal intensity and moderate FA values corresponding to desmoplasia (range 0.25 – 0.40) or fibrous tissue (range 0.28 – 0.41). Cancer was able to be distinguished from normal muscularis propria which was clearly anisotropic on DTI maps with high signal intensity and high FA (range 0.58 – 0.70). Figure 1 shows that DTI was able to identify demosplasia (B) and also cancer invasion into muscularis propria (C).

Figure Annotated regions are: **A** cancer **B** desmoplasia **C** cancer invasion into muscularis propria **D** fibrous tissue **E** uninvolved muscularis propria **F** uninvolved mucosa. The zoomed pathology image shows a region of cancer invasion into muscularis propria and desmoplasia

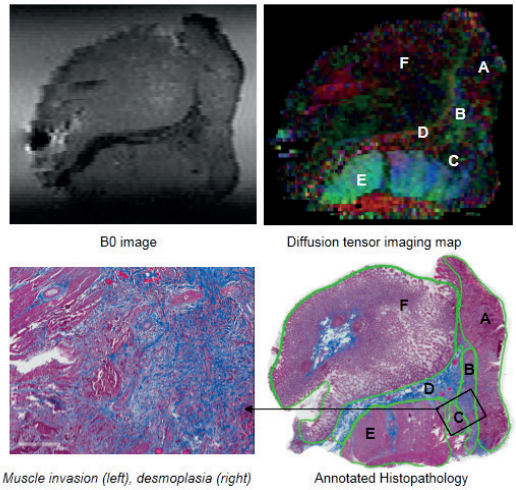

Conclusion

This exploratory study demonstrated DTI-MRI to be a feasible method of differentiating cancer regions from desmoplasia and fibrous tissue ex vivo. DTI was also able to identify cancer invasion into muscularis propria. DTI may add value in more accurately defining tumour extent in rectal cancer, and warrants further investigation.

[1]Beets-Tan et al Eur Radiol 2013:23:2522

PO-0980 Primary tumor and lymph nodes CT radiomics to predict loco-regional control in head and neck cancer

M. Bogowicz[1], O. Riesterer[1], G. Studer[1], J. Unkelbach[1], C. Schröder[1], M. Guckenberger[1], S. Tanadini-Lang[1]

[1]University Hospital Zürich, Radiation Oncology, Zurich, Switzerland

Purpose or Objective

Radiomics has shown a promise for predicting various endpoints in radiotherapy. So far radiomics-based models showed higher performance for endpoints referring directly to the primary tumor (local control) than for composite endpoints (loco-regional control and overall survival), which is potentially explained by most radiomics studies being based on the analysis of the primary tumor (PT) only. Here we hypothesize that loco-regional control (LRC) can be better predicted by a combination of the PT and involved lymph nodes radiomics.

Material and Methods

Head and neck squamous cell carcinoma patients treated with definitive radiochemotherapy were included in this retrospective study (training n = 81, validation n = 52). Details on the studied cohorts are presented in Table 1. Radiomics analysis was performed on contrast-enhanced planning CT with an in-house developed radiomics implementation. 567 features were extracted from both PT and lymph nodes (LN). Only lymph nodes defined as macroscopically involved (based on the biopsy or PET imaging) were included in the analysis. Principal component (PC) analysis combined with univariable Cox regression was used for selection of non-redundant features. Radiomic features were grouped according to correlation with PC and per group, only the feature with the highest prognostic power (concordance index CI) was selected as an input to multivariable model. The final model was trained using least absolute shrinkage and selection operator (100 times 10-fold cross validated).

Two models for prediction of LRC were trained. The first model (PT model) was based only on the PT radiomic features. In the second model (mixed model), the PT radiomics was first linked to local tumor control (LC) and the predictions obtained from this model were used as an input to LRC model together with LN radiomics. The performance of the two models was compared in the validation cohort based on the CI, using the Wilcoxon test ($p < 0.05$) and the bootstrap method with 100 randomly selected samples to calculate the CI distribution.